Characteristics of Earthquake Ground Motion on the Seafloor

Article *in* Journal of Earthquake Engineering · February 2015

DOI: 10.1080/13632469.2015.1006344

5 authors, including:

Dongsheng Wang
Hebei University of Technology
72 PUBLICATIONS **362** CITATIONS

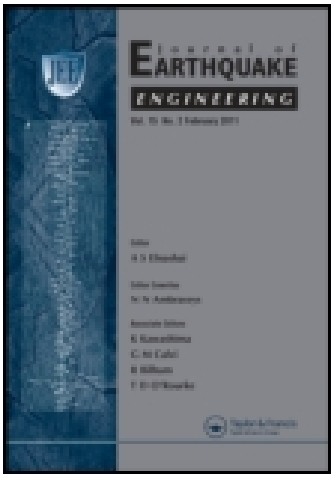

Journal of Earthquake Engineering
Publication details, including instructions for authors and subscription information:
http://www.tandfonline.com/loi/ueqe20

Characteristics of Earthquake Ground Motion on the Seafloor

Baokui Chen[a], Dongsheng Wang[a], Hongnan Li[a], Zhiguo Sun[b] & Yan Shi[b]

[a] Faculty of Infrastructure Engineering, Dalian University of Technology, Dalian, China

[b] Institute of Road and Bridge Engineering, Dalian Maritime University, Dalian, China

Accepted author version posted online: 11 Feb 2015.

Journal of Earthquake Engineering, 19:874–904, 2015

ISSN: 1363-2469 print / 1559-808X online
DOI: 10.1080/13632469.2015.1006344

Taylor & Francis
Taylor & Francis Group

Characteristics of Earthquake Ground Motion on the Seafloor

BAOKUI CHEN[1], DONGSHENG WANG[1], HONGNAN LI[1], ZHIGUO SUN[2], and YAN SHI[2]

[1]Faculty of Infrastructure Engineering, Dalian University of Technology, Dalian, China
[2]Institute of Road and Bridge Engineering, Dalian Maritime University, Dalian, China

The differences between onshore and offshore ground motions were studied based on the records from the K-net and SEMS. The horizontal response spectrum and vertical-to-horizontal response spectral ratio for offshore and adjacent onshore ground motions were analyzed. The results indicate that the characteristic period of the response spectra for offshore ground motions is obviously larger. The epicentral distance can influence the horizontal response spectra for offshore ground motions in a moderate earthquake, while the influence of water depth is not noticeable. Moreover, the vertical–to-horizontal response spectral ratio for offshore ground motions is significantly smaller for periods less than 1 s.

Keywords Offshore Ground Motion; Onshore Ground Motion; Elastic Response Spectrum; Vertical-to-Horizontal Response Spectral Ratio; Vertical-to-Horizontal PGA Ratio; K-net Network; Seafloor Earthquake Measuring System

1. Introduction

The construction of offshore structures, such as oil platforms, cross-sea bridges, submarine tunnels, artificial islands, and floating structures is becoming more commonplace. Despite their commonness, these offshore structures are vulnerable to strong earthquakes. In 1989, for example, the girders of the San Francisco-Oakland Bay Bridge fell down during the Loma Prieta earthquake; this led to traffic over the bridge being closed for weeks [Nolen-Hoeksema and Morrow, 1991]. In addition, in 1995, the Kobe earthquake resulted in the damage of two offshore artificial islands, Port Island and Rokko Island, due to the liquefaction of the reclaimed fills [Tanaka, 2000]. Consequently, research on the characteristics of ground motion on the seafloor is important to ensure the safety of offshore structures during earthquakes.

Despite the fact that many offshore structures have been and are being constructed in moderate to high seismicity regions, few studies have characterized the offshore ground motion, owing to a lack of strong motion records at offshore stations. Commonly, earthquake design loads developed from onshore ground motion records are used for offshore structure design.

Received 19 August 2013; accepted 31 December 2014.

Address correspondence to Dongsheng Wang, Faculty of Infrastructure Engineering, Dalian University of Technology, Dalian 116024, China. E-mail: dswang@dlmu.edu.cn

Color versions of one or more of the figures in the article can be found online at www.tandfonline.com/ueqe.

When considering the seismic design of structures, it should be noted that the response spectrum plays an important role. Chopra [2007] reviewed the origin and early development of the elastic response spectrum. Although the response spectrum for onshore ground motion had been extensively studied, research on the response spectrum for offshore ground motion is lacking.

Boore and Smith [1999] analyzed the vertical-to-horizontal spectral ratio of ground motions from eight earthquakes at five offshore sites recorded by the Seafloor Earthquake Measuring System (SEMS) project in the United States. The results indicated that offshore ground motion had a very low vertical component, as compared to onshore motions, particularly at short periods. Unfortunately, the research did not select the records at both onshore and offshore sites during the same earthquake event. Atakan and Havskov [1996] evaluated site response using the horizontal-to-vertical spectral ratio from the temporary ocean bottom seismograph (OBS) network in the northern North Sea and a permanent OBS at the Oseberg oil field. In their study the Single Station Spectral Ratio (SSSR) method developed by Nakamura [1989] appears to work well in estimating the local site response in a marine environment.

In this article, the ground motion data for six offshore and eight adjacent onshore stations during six earthquake events in the K-net strong-motion seismograph network were collected with the purpose of analyzing the differences in the characteristics between onshore and offshore ground motions. In addition, data from five offshore stations during eight earthquake events from the SEMS project were used to confirm the research findings from the K-net data. The data from the SEMS project are consistent with the study of Boore and Smith [1999].

The horizontal response spectra, the vertical-to-horizontal PGA ratio (V/H PGA ratio) and the vertical-to-horizontal response spectral ratio (V/H RS ratio) for offshore ground motions were investigated and compared with those of onshore ground motions. The conclusions of this research may provide better guidance for the seismic design of offshore structures.

2. Ground Motion Records

The ground motion records are selected from the K-net strong-motion seismograph network and the SEMS project.

2.1. K-net Network and the SEMS Project

The K-net (Kyoshin network), where Kyoshin is the Japanese word that means strong-motion, is a nationwide strong-motion seismograph network located throughout Japan [Aoi *et al.*, 2004; Okada *et al.*, 2004]. Japan is in the circum-Pacific seismic belt and most of earthquakes belong to plate-margin earthquakes. More than 1000 stations were set up covering the whole of Japan with spacing within 25 km to immediately provide obtained data under an open policy. The K-net database was built by the National Research Institute for Earth Science and Disaster Prevention in Japan. The Japanese Meteorological Agency provides such information as origin time, epicentral distance, and magnitude. All ground motion data and site information since 1996 can be obtained on the K-net website (http://www.kyoshin.bosai.go.jp/). The records from the K-net have been studied by many researchers around the world [Lussou *et al.*, 2001; Pousse *et al.*, 2005]. This study selected ground motion records from six offshore and eight onshore stations in the K-net. These earthquake stations are located in the southern Kanto region, where earthquakes occur frequently and earthquake stations are densely distributed.

Originally, the strong-motion seismograph (K-NET95) used in the K-net was three component accelerograph. After 2004, the current strong-motion seismograph (K-NET02) replaced the old one. The main features of the new strong-motion seismograph are functions for processing JMA (Japan Meteorological Agency) seismic intensity and nearly real time data communications. The maximum measurable acceleration is improved from 2000 to 4000 gal. The dynamic range of an AD conversion is 132 dB and the sampling frequency is 100 Hz [Fujiwara *et al.*, 2004].

The SEMS project was built on the seafloor at offshore sites of southern California, near oil platforms. The SEMS instrument development, deployment, and data recovery were carried out by Sandia National Laboratory, with funding from the Minerals Management Service. A three-axis accelerometer was embedded several meters below the seafloor. The data acquisition units for the first three SEMS stages used 16-bit digitizing at 100 samples per second and the forth SEMS4 unit used 24-bit digitizing at 20 samples per second [Smith, 1994; Boore and Smith, 1999].

2.2. Records Selection and Data Processing

There are six offshore strong-motion stations (KNG201–KNG206) in the K-net. These offshore stations are spaced 10–20 km apart in Sagami Bay. The water depth at the offshore sites is between 900 and 2300 m. The detailed information about the onshore and offshore stations is provided in Table 1. A map showing the locations of the six offshore stations (KNG201–KNG206) and the eight onshore stations (CHB017, KNG008, SZO001, SZO002, SZO007, TKY008, TKY009, and TKY010) used for this article is given in Fig. 1; of these six white triangles represent the offshore stations and eight black dots represent the onshore stations.

This study selected 36 offshore and 31 onshore ground motions from the K-net. Information about onshore and offshore ground motions is provided in Appendix A. The ground motions are selected from six earthquake events between 2006 and 2012, with

TABLE 1 Information of onshore and offshore stations in the K-net network

Site No.	Site name	Lat.	Long.	Water depth (m)
KNG201	HIRATSUKA-ST1	34.5956N	139.9183E	2197
KNG202	HIRATSUKA-ST2	34.7396N	139.8393E	2339
KNG203	HIRATSUKA-ST3	34.7983N	139.6435E	902
KNG204	HIRATSUKA-ST4	34.8931N	139.5711E	933
KNG205	HIRATSUKA-ST5	34.9413N	139.4213E	1486
KNG206	HIRATSUKA-ST6	35.0966N	139.3778E	1130
CHB017	ICHIBA	35.2988N	140.0755E	Onshore
KNG008	SAGAMIHARA	35.5751N	139.3265E	Onshore
SZO001	ATAMI	35.1424N	139.0795E	Onshore
SZO002	ITOH	34.9652N	139.1031E	Onshore
SZO007	SHUZENJI	34.9771N	138.9466E	Onshore
TKY008	OKADA	34.7852N	139.3909E	Onshore
TKY009	HABUMINATO	34.6874N	139.4412E	Onshore
TKY010	NIIJIMA	34.3779N	139.2573E	Onshore

*The data in the table can be found on the website: http://www.kyoshin.bosai.go.jp/.

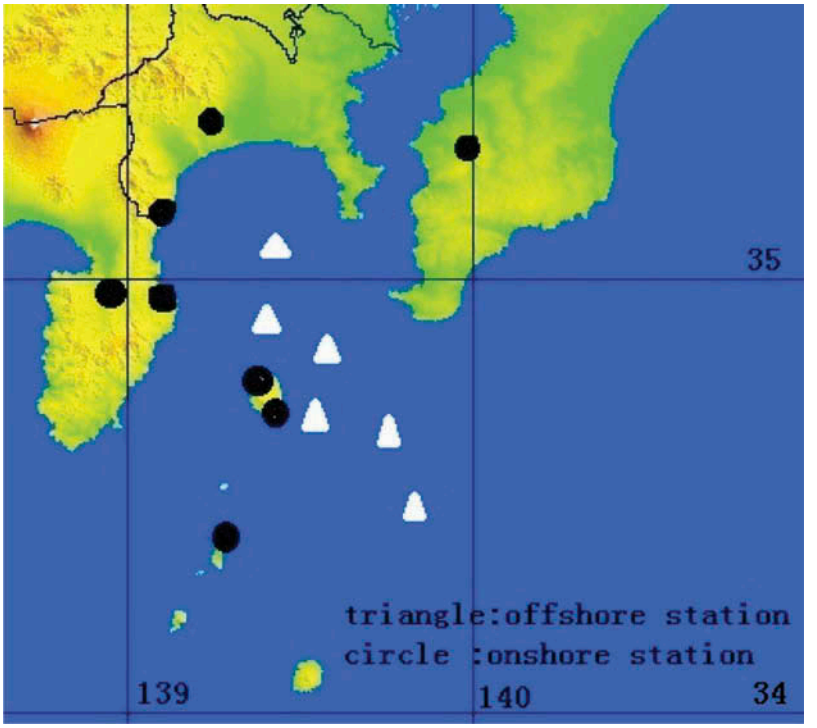

FIGURE 1 Locations of onshore and offshore stations used in this study from the K-net.

TABLE 2 Information of six earthquake events in the K-net network

Eq. location	Data	Time	Lat.	Long.	M_w	Hypocenter depth (km)	Epicentral site
Izu Peninsula	2006-04-21	02:50	34.940N	139.195E	5.8	7	Seafloor
Sagami Bay	2006-05-02	18:24	34.917N	139.330E	5.1	15	Seafloor
Suruga Bay	2009-08-11	05:07	34.785N	138.498E	6.5	23	Seafloor
Tohoku	2011-3-11	14:46	38.103N	142.860E	9.0	24	Seafloor
Mount Fuji	2011-03-15	22:31	35.308N	138.713E	6.4	14	Land
Tokyo Bay	2012-07-03	22:31	35.000N	139.870E	5.2	88	Land

*The data in the table can be found on the website: http://www.kyoshin.bosai.go.jp/.

magnitudes between M_w 5.1 and M_w 9.0. Each ground motion record contains one vertical component and two horizontal components. The hypocentral depth of 6 earthquakes is less than 25 km, except for the Tokyo Bay earthquake on July 3, 2012 with a hypocentral depth of 88 km. Information on the six earthquake events is summarized in Table 2.

For each earthquake event, six offshore ground motions and five or six onshore ground motions were selected. In order to compare the differences between onshore and offshore ground motions effectively, the onshore stations were selected based on the following criteria: (a) the onshore stations should be close to the offshore stations; (b) the onshore sites should be on stiff soil site and the average shear-wave velocity should be 180–360 m/s; (c) the same onshore stations should be selected for all earthquakes, which can effectively compare the onshore and offshore ground motions for different earthquakes; and (d) the

PGA of horizontal ground motions should be larger than 30 gal in order to have effective data. Therefore, eight onshore stations were selected to provide the onshore ground motion records for this study.

The ground motion records at five offshore stations during eight earthquake events in the SEMS project were selected (another two offshore stations have not selected records). In each earthquake event, data were recorded at only one offshore station except one, in which two offshore stations obtained the data. The earthquake magnitudes range from M_w 4.7 to M_w 6.1. Because of a scarcity of multiple records at both onshore and offshore stations during one earthquake event, only offshore ground motions were selected from the SEMS project to study the characteristics of ground motions on the seafloor. The information about the offshore stations in the SEMS is listed in Table 3. The earthquake events selected are summarized in Table 4. Information about offshore ground motions in the SEMS is provided in Appendix B.

These ground motion records were corrected for filtering and baseline correction by public software of SeismoSignal. The SeismoSignal provides an easy and efficient way to process strong-motion data and was used by hundreds of international academics and research institutions [Mendes and Lourenço, 2009; KomakPanah and Bagheri, 2013]. The original data were filtered by a 4-order Butterworth filter to remove the low frequency parts of the record contaminated by long period noise; the frequencies range between 0.1 and 25 Hz. In some cases, baseline adjustments can be used in conjunction with filters to provide optimum record processing. The linear polynomial curve method was used for baseline correction. Detailed information can be obtained on the website (www.seismosoft.com), help menu in the software, and a technical literature [Boore and Bommer, 2005] recommend by SeismoSignal.

TABLE 3 Information of offshore stations in the SEMS project

Station	Lat.	Long.	Water depth (m)
S1HN	34.3367N	119.5600W	50
S2EE	33.5867N	118.1233W	73
S3EE	33.5700N	118.1300W	64
S4GR	34.1800N	119.4700W	99
S4IR	34.6117N	120.7300W	76

TABLE 4 Information of earthquake events in the SEMS project

Eq. ID	Eq. Name	Date	Time	Lat.	Long.	M_w	Epicentral site
SB81	Santa Barbara Island	1981-09-04	15:50	33.66N	119.10W	5.95	Seafloor
NP86	North Palm Springs	1986-07-08	09:20	34.00N	116.61W	6.10	Land
OS86	Oceanside	1986-07-13	13:47	32.97N	117.87W	5.84	Seafloor
UP90	Upland	1990-02-28	23:43	34.14N	117.70W	5.63	Land
RC95	Ridgecrest	1995-09-20	23:27	35.76N	117.64W	5.56	Land
CL97	Calico	1997-03-18	15:24	34.97N	116.82W	4.85	Land
S97A	Simi Valley	1997-04-26	10:37	34.37N	118.67W	4.81	Land
S97B	Simi Valley	1997-04-27	11:09	34.40N	118.64W	4.72	Land

2.3. Site Conditions

The K-net strong-motion seismograph network provides information about soil and geological structures at onshore sites. Each site provides geotechnical characteristic, such as P–wave and S–wave logs, and standard penetration test values. Soil layer information is obtained by drilling 10–20 m underground. Figure 2 illustrates the distribution of the soil layers and shear-wave velocity at one K-net site SZO002. The total depth of soil layer (H) is different for each K-net site and ranges from 10–20 m. The average shear-wave velocity ($\bar{V}_{s)}$ is thus calculated as

$$\bar{V}_s = \frac{\mathrm{H}}{\sum \frac{\mathrm{h}_i}{V_{si}}}, \tag{1}$$

where $\bar{V}_s$ is the average shear-wave velocity, H is the total depth of the soil layer, h_i is the depth of each soil layer, and V_{si} is the shear-wave velocity of each soil layer.

Unfortunately, information about the soil layer at offshore sites is not available in the K-net. Only a limited amount of information about offshore site condition can be found in some references. Takao *et al*. [1998] carried out a site survey. It illustrated that the maximum inclination angle of the seafloor across the offshore sites in the K-net was approximately less than ten degrees. Most of the offshore sites are underlain by sediments consisting of sand, small-sized pebbles or small-sized rock, not by soft or unconsolidated sediments with a small S-wave velocity.

Based on the sediment components, the offshore sites seem to be stiff soil sites according to the experiences on land; however, it should be noted that the water layer will increase the pore pressure in the sediments, which will reduce the shear-wave velocity in sand and silt sites [Boore and Smith, 1999].

Otsuka [1985] made an exploration test and conducted that the Sagami geological layer belongs to the Quaternary pluvial period strata, the top of this geological layer covers a deep deposition layer. The main components of the deposition layer include sludge soil, sediment containing coarse sand, graded sand, and a silty sand layer. Although the seafloor

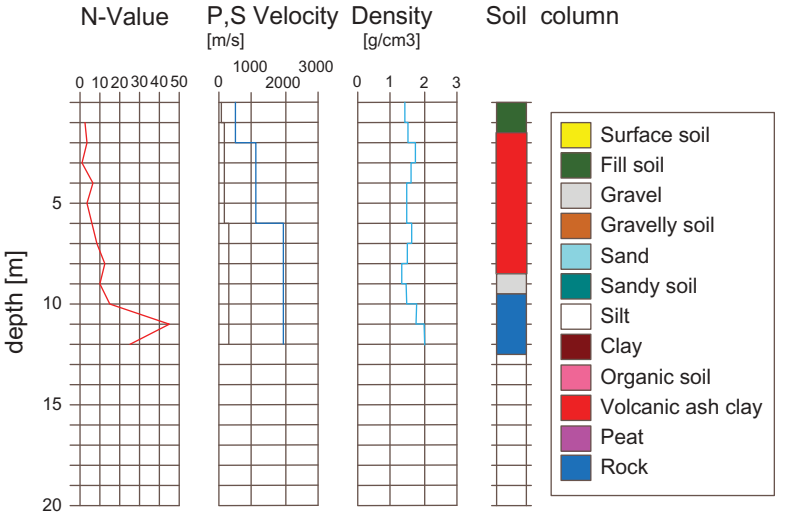

FIGURE 2 The distribution of soil layer at onshore site SZO002.

compliance method can indirectly calculate the shear-wave velocity [Crawford *et al.*, 1991], this method cannot be used on the seabed in Sagami Bay; this is due to a lack of data such as seafloor pressure.

The average shear-wave velocity for the onshore sites near Sagami Bay in the K-net (not only some of the onshore sites mentioned previously, but also other sites at the shoreline near this region) is between 90 and 380 m/s. The mean value is about 230 m/s.

The average shear-wave velocity of the SEMS offshore sites was speculated to be about 220 m/s [Boore and Smith, 1999].

3. Analysis of Elastic Response Spectrum

Figures 3–5 show the distribution of the horizontal PGA of onshore and offshore ground motions in the K-net for different earthquake magnitudes, epicenter distances, and hypocentral depths. These figures indicate that the distribution of the PGA between onshore and offshore ground motions is homogeneous. Thus the study of the differences between onshore and offshore ground motions would not be affected by PGA.

Because there are no corresponding onshore ground motion records and because the PGA for all offshore ground motions in the SEMS is less than 30 gal, the PGA in the SEMS have not been illustrated in Figs. 3–5.

Figure 6 shows the relationship between the magnitude and epicentral distance for ground motion records in the K-net and SEMS. This figure also illustrates that most of the K-net data consist of earthquake events with magnitudes between M_w 5.1 and M_w 6.5 and epicentral distances less than 136 km; that being said, the epicentral distance and magnitude of the Tohoku earthquake on March 11, 2011 is significantly larger. Furthermore, only offshore data are included in the SEMS consisting of events with magnitudes between M_w 4.7 and M_w 6.1 and epicentral distances between 72 and 310 km.

Differences in the elastic response spectra between onshore and offshore ground motion were analyzed. The response spectra used in this article are the normalized response spectrum. A normalized response spectrum (amplification factor spectrum) is obtained by a spectral acceleration divided by the corresponding PGA. The equation can be illustrated as follows:

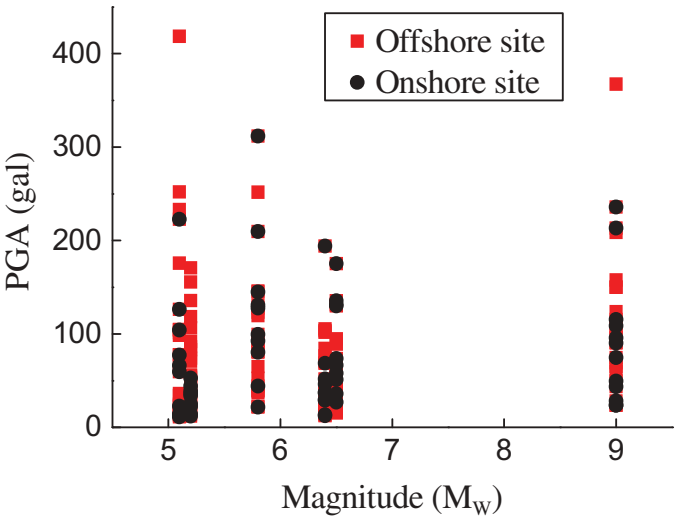

FIGURE 3 PGA vs. Magnitude of the horizontal accelerograms for onshore and offshore ground motions used in this paper from the K-net.

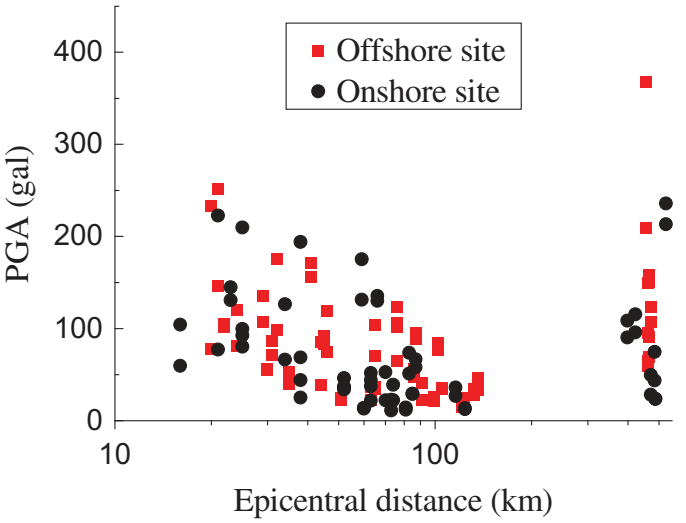

FIGURE 4 PGA vs. Epicentral distance of the horizontal accelerograms for onshore and offshore ground motions used in this paper from the K-net.

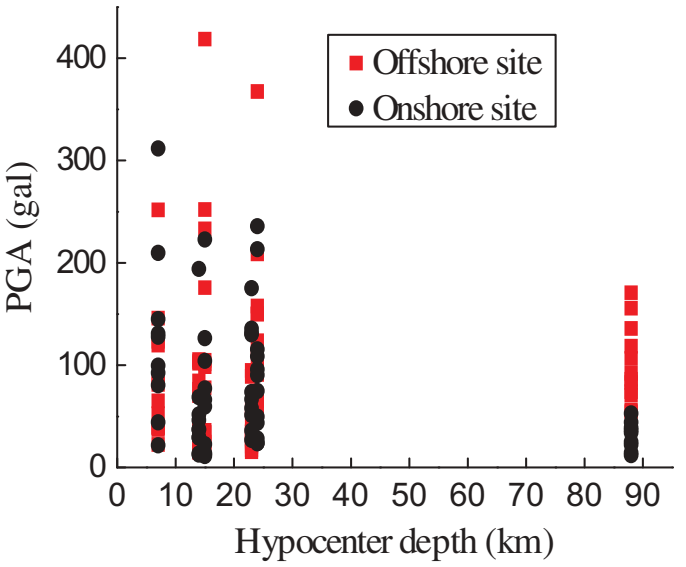

FIGURE 5 PGA vs. Hypocenter depth of the horizontal accelerograms for onshore and offshore ground motions used in this paper from the K-net.

$$\beta_{\mathrm{a}} = \frac{S_a}{a} \tag{2}$$

where β_a is the amplification factor, S_a is the spectral acceleration, and a is the PGA.

When some ground motions are used to calculate an average response spectrum, a statistical coefficient of variation is presented to measure the statistical dispersion of the results. The coefficient of variation can be calculated as the standard deviation divided by the mean value. The coefficient of variation of a normalized response spectrum changes along with the periods.

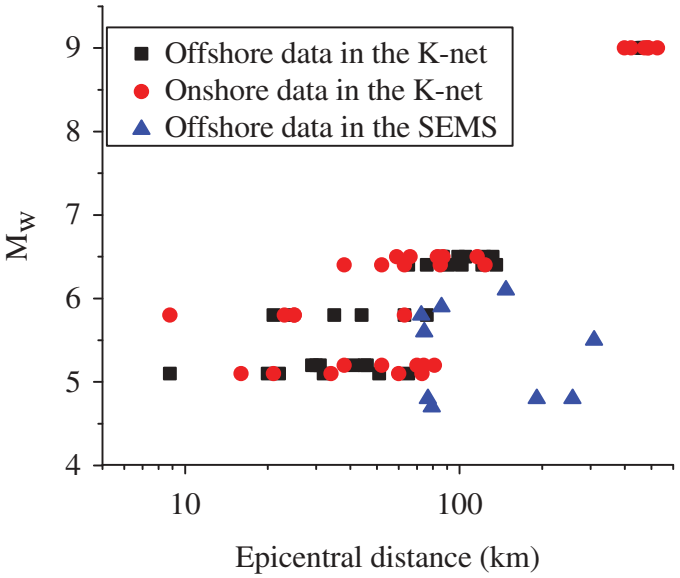

FIGURE 6 Magnitude vs. Epicentral distance of ground motions used in this paper.

3.1. Horizontal Response Spectrum

Data for 36 offshore and 31 onshore ground motions were selected from 6 earthquakes in the K-net, and each ground motion included 1 vertical and 2 horizontal components. These records were used to analyze the differences in the horizontal normalized response spectra between onshore and offshore ground motions. The periods of the normalized response spectra range between 0.05 and 5.0 s; the damping ratio is taken to be 5%. The response spectra and its corresponding coefficient of variation for onshore and offshore ground motions in the 6 earthquakes are shown in Figs. 7–12.

As illustrated in Figs. 7a–12a, the response spectra (normalized response spectra) for ground motions between the different earthquake events were similar, but the differences

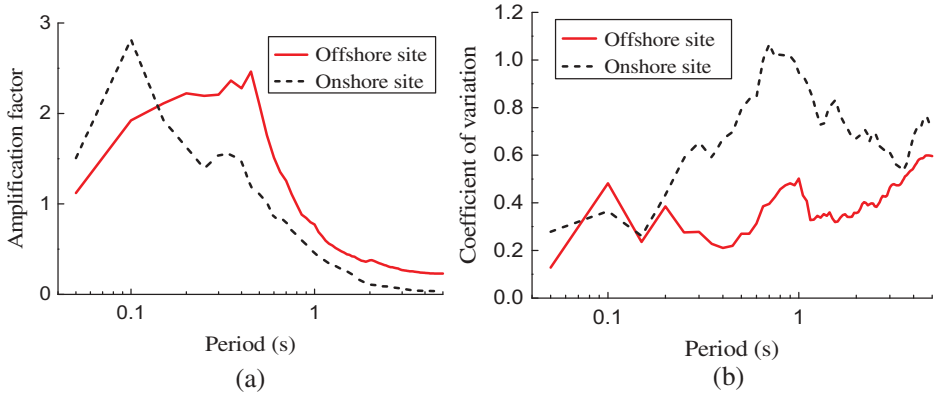

FIGURE 7 Horizontal response spectra (amplification factor spectra) for onshore and offshore ground motions from the K-net in the earthquake on April 21, 2006 and corresponding coefficient of variation.

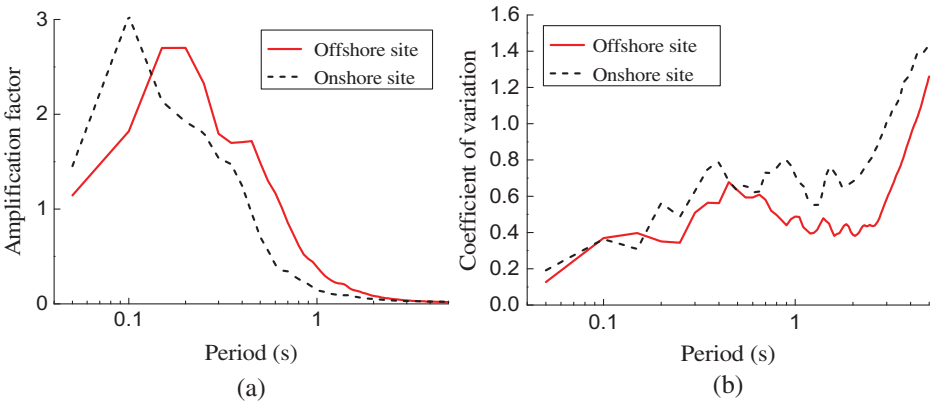

FIGURE 8 Horizontal response spectra for onshore and offshore ground motions from the K-net in the earthquake on May 2, 2006 and corresponding coefficient of variation.

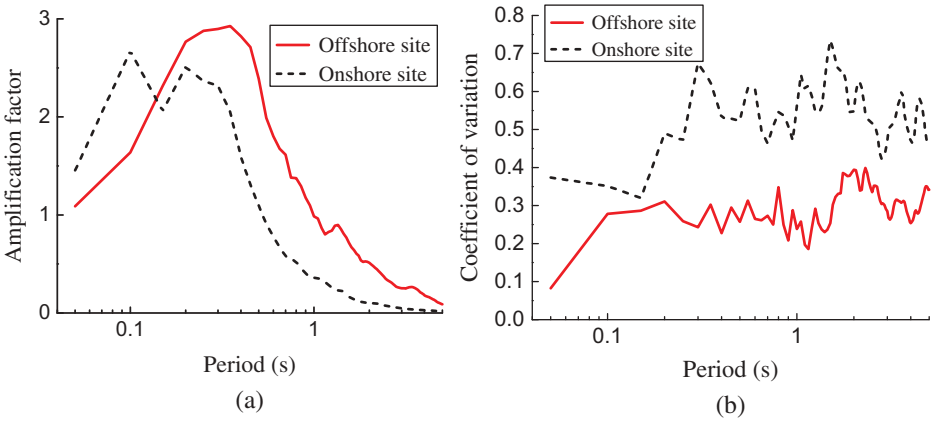

FIGURE 9 Horizontal response spectra for onshore and offshore ground motions from the K-net in the earthquake on August 11, 2009 and corresponding coefficient of variation.

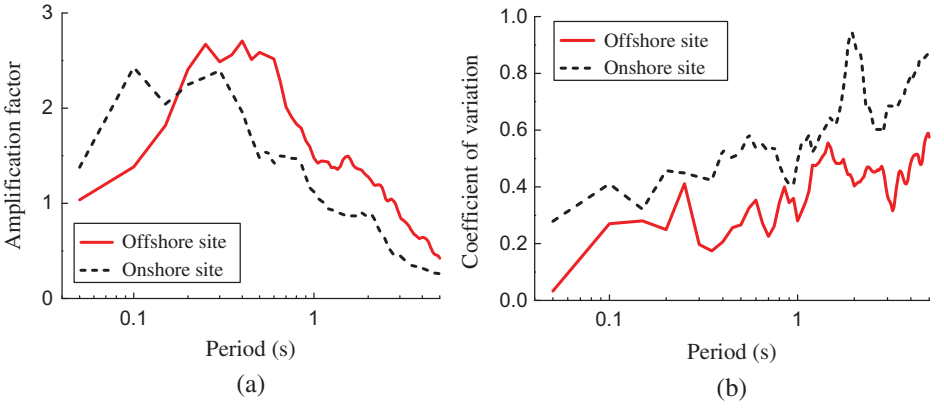

FIGURE 10 Horizontal response spectra for onshore and offshore ground motions from the K-net in the earthquake on March 11, 2011 and corresponding coefficient of variation.

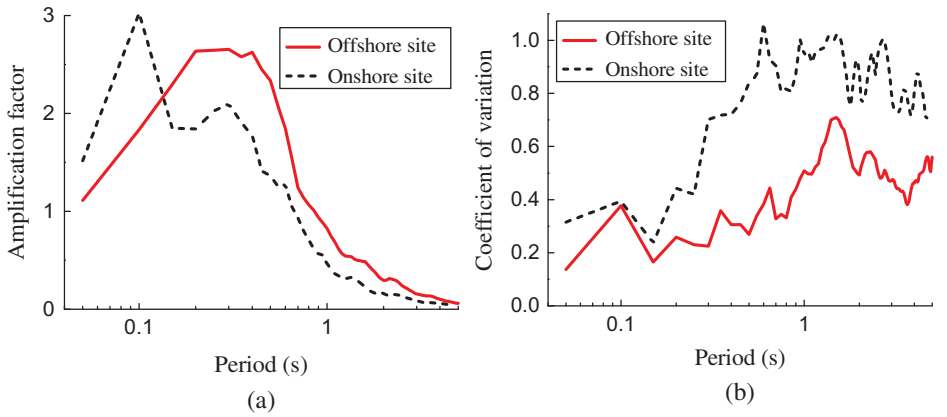

FIGURE 11 Horizontal response spectra for onshore and offshore ground motions from the K-net in the earthquake on March 15, 2011 and corresponding coefficient of variation.

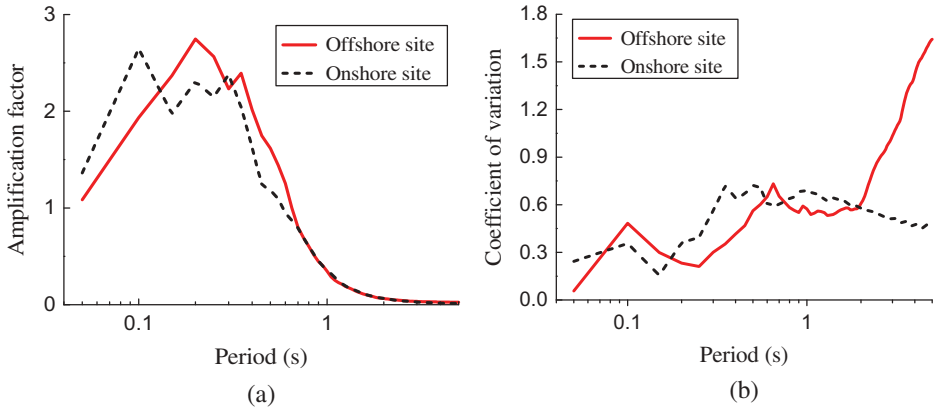

FIGURE 12 Horizontal response spectra for onshore and offshore ground motions from the K-net in the earthquake on July 3, 2012 and corresponding coefficient of variation.

between the onshore and offshore motions were obvious, which can be summarized as follows. For short periods less than 0.1 s, the response spectra for offshore ground motions were lower than that of onshore ground motions, and an intersection exists for the response spectra between onshore and offshore ground motions for periods between 0.1 and 0.2 s. For periods longer than 0.2 s, the response spectra for offshore ground motions were larger than that of onshore ground motions. The characteristic period of response spectra for onshore ground motions was between 0.2 and 0.3 s; and that for offshore ground motions was between 0.5 and 0.6 s. For periods longer than 1 s, the spectral values were less than 1.0 for both onshore and offshore ground motions, and the spectral values of offshore ground motions were still larger than those of onshore ground motions.

When comparing to the onshore ground motions, there is an obvious peak platform for the response spectrum of offshore ground motions. It clearly indicates that the characteristic period of response spectra for offshore ground motions is larger than that of onshore ground motions.

The average response spectra (normalized response spectra) for all onshore and offshore ground motions from the 6 earthquakes in the K-net and the response spectrum

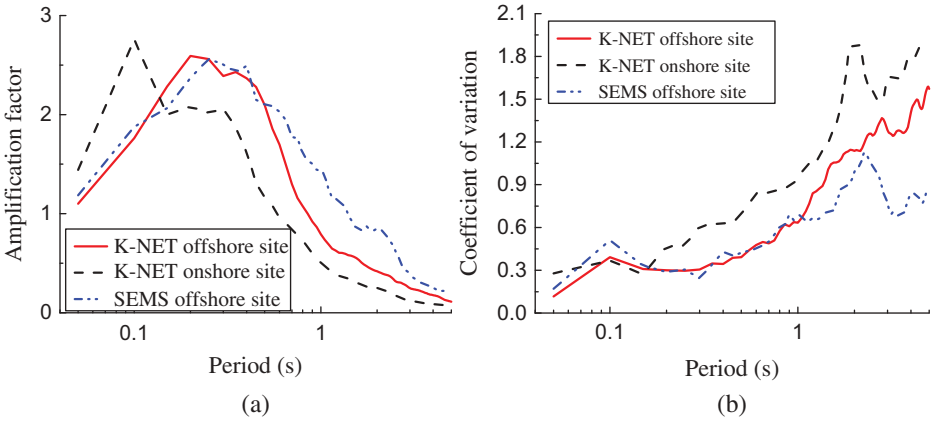

FIGURE 13 Average horizontal response spectra for ground motions from the K-net and SEMS and corresponding coefficient of variation.

for offshore ground motions in the SEMS are compared in Fig. 13a. As shown in Fig. 13a, the characteristics of the response spectra for offshore ground motions from the K-net were consistent with those of the SEMS. The water depth of the offshore stations in the K-net (between 900–2300 m) is significantly larger than that in the SEMS (50–100 m). The results indicate that the water depth seems to have little influence on the horizontal response spectra.

As mentioned above, a water layer will increase the pore pressure to reduce the velocity at offshore sites. In addition, the Sagami geological layer where the six K-net offshore stations located may cover a deep deposition layer. Therefore, the filtering effect of soil layer under seafloor may be the reason that the offshore ground motions have longer period contents compared to the onshore ground motions, as same as the soft soil effect on the spectra at onshore sites. The response spectra for offshore ground motions in Figs. 7a–13a were larger than that of onshore ground motions at long periods. This result is similar to the characteristics of the response spectra for onshore ground motions at soft soil sites.

Boore and Smith [1999] also concluded that the water layer had little effect on the horizontal component of offshore ground motion. A deep low-velocity deposition layer is commonly covered on the seafloor in the SEMS; the soft sediments would influence the horizontal ground motion at long periods.

For the Tohoku earthquake (March 11, 2011), the spectral values of offshore ground motions are obviously larger than the other earthquakes for periods longer than 1.0 s. The reasons may be related to the great earthquake magnitude ($M_w = 9.0$) and far epicentral distances (more than 400 km).

The statistical coefficients of variation of the normalized response spectra are shown in Figs. 7b–13b. The coefficients of variation were found to be similar at both onshore and offshore sites; these coefficients increased with the periods. The coefficient of variation of onshore data was larger than that of offshore data, especially for long periods. For periods less than 2 s, the coefficients of variation of onshore and offshore data were usually smaller than 1.0. This means the statistical dispersion of the data can be accepted.

3.2. Influence of the Epicentral Distance

The epicentral distance is an important influential factor of the response spectra for ground motions. Due to a lack of offshore records, the influence of the epicentral distance on the

response spectra for offshore ground motions cannot be studied in the same earthquake event. In this study, most of ground motion records in the K-net were collected from moderate earthquake events with magnitudes between M_w 5.1 and M_w 6.5 and epicentral distances less than 140 km. Therefore, the influence of the epicentral distance on the response spectra is mostly discussed in a moderate earthquake, except in the case of the offshore data in the Tohoku earthquake (M_w 9.0 earthquake with far-field distances more than 400 km).

The ground motions in the K-net were classified into 3 groups, according to their earthquake magnitudes and epicentral distances R: (1) MSR (moderate earthquake, small distance, $R < 30$ km); (2) MMR (moderate earthquake, medium distance, $30 \leq R < 140$ km); and (3) GFR (great earthquake, $M_w = 9.0$; far distance, $R \geq 400$ km). Furthermore, the offshore ground motions in the SEMS were classified into one group, as most of the offshore ground motions were in moderate earthquakes with epicentral distances between 70 and 310 km.

Generally, both site condition and earthquake magnitude would affect the response spectrum. Unfortunately, the geological information at offshore sites cannot be obtained. In addition, only one great earthquake (the Tohoku earthquake) with a magnitude of M_w 9 was selected. Consequently, we classify the records as discussed previously.

The response spectra (normalized response spectra) for onshore and offshore ground motions in MSR, MMR, and GFR groups are compared respectively in Figs. 14a–16a. The differences in the response spectra between the onshore and offshore ground motions are consistent with the characteristics of response spectra in Figs. 7a–13a. The response spectra for offshore ground motions were found to have a wider peak platform and greater spectral values at long periods with increasing epicentral distances. The characteristic periods of the response spectra for offshore ground motions in MSR, MMR, and GFR groups were about 0.2 s, 0.5 s, and 0.6 s, respectively.

When the average response spectra were calculated by the above ground motion classifications, the statistical coefficients of variation of the response spectra are smaller than 1.2 in Figs. 14b–16b, which are smaller than those in Figs. 7b–13b at long periods.

The normalized response spectra of offshore ground motions for three groups from the K-net and one group from the SEMS are shown in Fig. 17a. The spectral values for offshore ground motions in the SEMS was larger than those for offshore ground motions in the MSR and MMR groups for periods longer than 0.5 s. Because the magnitudes of

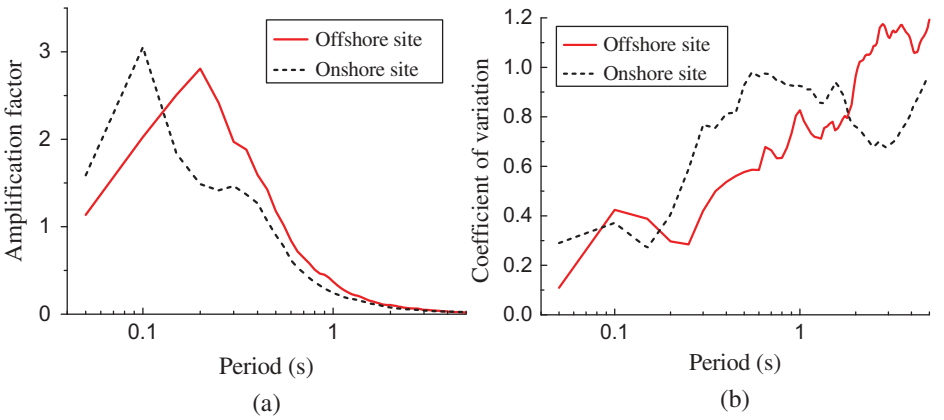

FIGURE 14 Horizontal response spectra for onshore and offshore ground motions in MSR group and corresponding coefficient of variation.

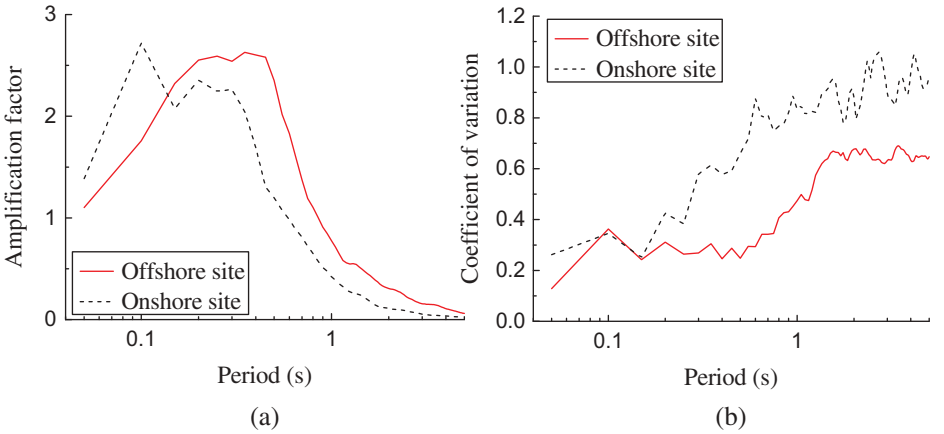

FIGURE 15 Horizontal response spectra for onshore and offshore ground motions in MMR group and corresponding coefficient of variation.

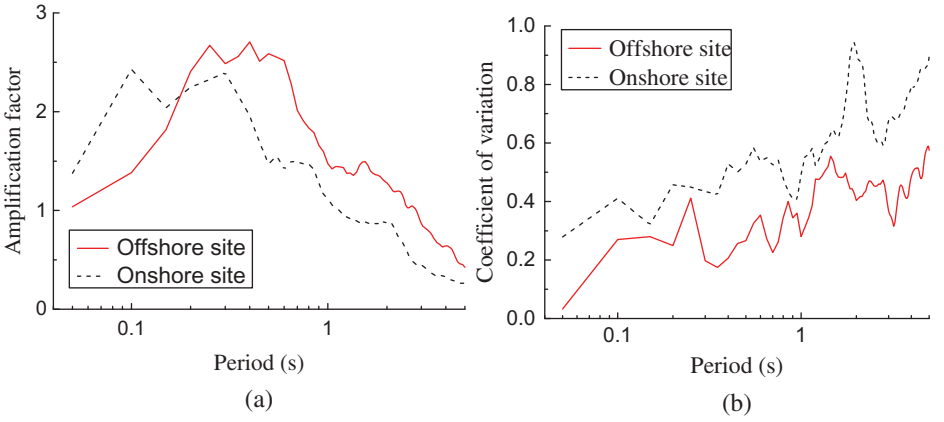

FIGURE 16 Horizontal response spectra for onshore and offshore ground motions in GFR group and corresponding coefficient of variation.

most of the data in the SEMS belong to moderate earthquake and the epicentral distances are from 70–310 km (R is larger than that in the MSR and MMR). This indicates that the influence of the epicentral distance on the response spectra for offshore ground motions is obvious in a moderate earthquake; with increasing epicentral distances, the spectral values for offshore ground motions will be larger at long periods.

As shown in Fig.17a, the spectral values in the GFR group are larger than those in the MSR and MMR groups for periods longer than 0.6 s. This illustrates that the offshore ground motions in a great earthquake with far epicentral distance have longer period (lower frequency) contents.

4. Vertical Ground Motion

Recently, seismic damage investigations have revealed that some structures were destroyed by vertical ground motion in some earthquakes such as the Northridge earthquake in 1994 and the Kobe earthquake in 1995 [Hashimoto and Chouw, 2003; Elgamal and He,

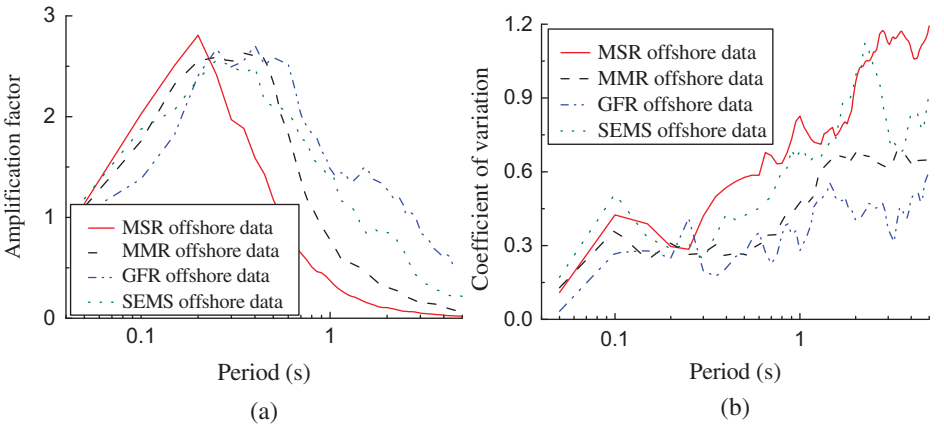

FIGURE 17 Horizontal response spectra for offshore ground motions with different epicentral distances from the K-net and SEMS and corresponding coefficient of variation.

2004]. Many researchers have studied the response spectrum of the vertical ground motion at onshore sites [Dimitriu *et al.*, 1999; Bozorgnia *et al.*, 2000; Ambraseys and Douglas, 2003; Yanf and Lee, 2007; Kim *et al.*, 2010; Bindi *et al.*, 2010], but research on the vertical ground motion at offshore sites still remains limited. Boore and Smith [1999] studied the vertical-to-horizontal response spectral ratio at offshore sites. Due to limitations in the layout of the earthquake stations, the research did not find adequate ground motion records at both onshore and offshore sites during the same earthquake event.

The vertical-to-horizontal peak ground acceleration ratio (V/H PGA ratio) and the vertical-to-horizontal response spectral ratio (V/H RS ratio) were investigated to determine the characteristics of vertical ground motions on the seafloor in this research.

4.1. Vertical Peak Ground Acceleration

Figure 18 compares the accelerograms recorded at offshore station (KNG201) and onshore station (KNG008) during the Tohoku earthquake. The accelerograms were randomly selected from the K-net. The PGA of the horizontal accelerograms were found to be between 110 and 120 gal at both onshore and offshore stations, but the PGA of the vertical accelerogram at offshore station is only about 15 gal (48 gal at onshore station). The vertical PGA at offshore sites is lower than that at onshore sites.

In order to compare the differences in vertical PGA between onshore and offshore ground motions, the vertical-to-horizontal peak ground acceleration ratio ($_{\text{V/H PGA ratio}}$) is calculated as follows:

$$\Delta = {}^{V_A}/_{H_A}, \tag{3}$$

where $\triangle$ is the vertical-to-horizontal PGA ratio, V_A is the vertical PGA, and H_A is the horizontal PGA.

After calculating the average V/H PGA ratio for all onshore and offshore ground motions in the K-net, it was found that the average V/H PGA ratio for offshore ground motions was 0.223; the ratio for onshore ground motions was 0.474. Figures 19 and 20 show the relationship between the vertical and horizontal PGA values for onshore and

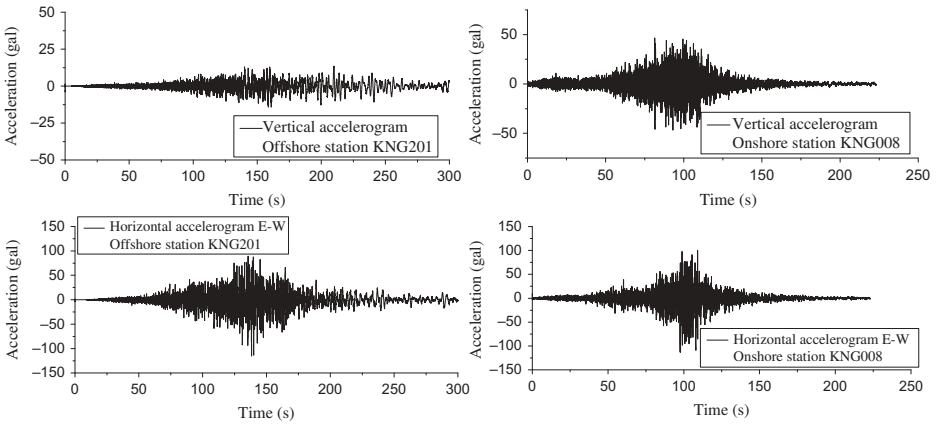

FIGURE 18 Comparison of vertical and horizontal accelerograms between onshore site KNG008 and offshore site KNG201 for the earthquake on March 11, 2011, of which the horizontal accelerograms are in East-West direction.

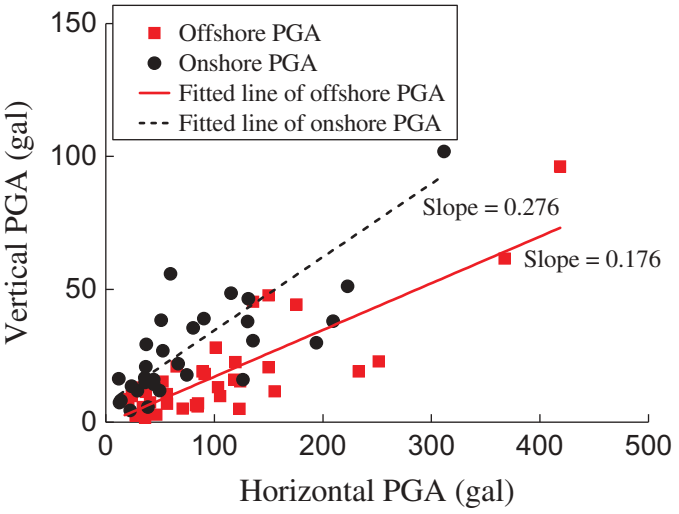

FIGURE 19 Relationship between the vertical and horizontal (E–W) PGA values for onshore and offshore ground motions in the K-net.

offshore ground motions in the K-net. A linear fitting is made with the vertical and horizontal PGA values and shown in Figs. 19 and 20. For offshore ground motions, the slope of the fitting line of vertical and horizontal (E–W) PGA is 0.176; and it is 0.265 for the vertical and horizontal PGA (S–N). For onshore ground motions, the slope of the fitting line for the vertical and horizontal (E–W) PGA is 0.276; it is 0.429 for the vertical and horizontal PGA (S–N).

The PGA for ground motions depends on the epicentral distance and the earthquake magnitude, so the influence of epicentral distance and earthquake magnitude on the V/H PGA ratio is also discussed. Figure 21 presents the relationship between the epicentral distance and the V/H PGA ratio for offshore ground motions in the K-net. The V/H PGA

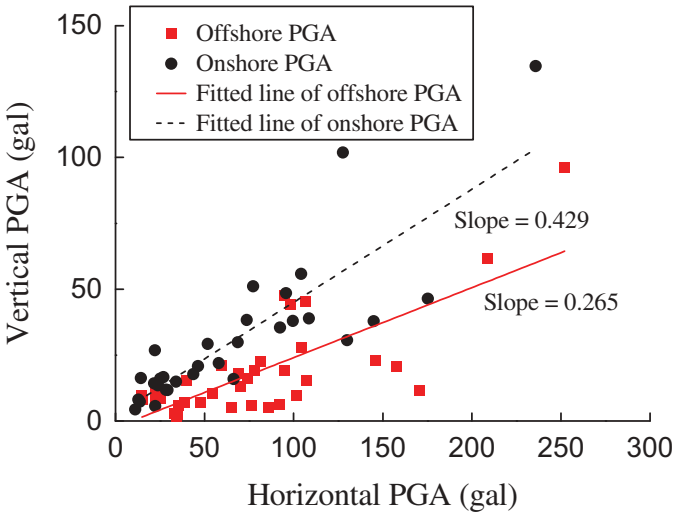

FIGURE 20 Relationship between the vertical and horizontal (N–S) PGA values for onshore and offshore ground motions in the K-net.

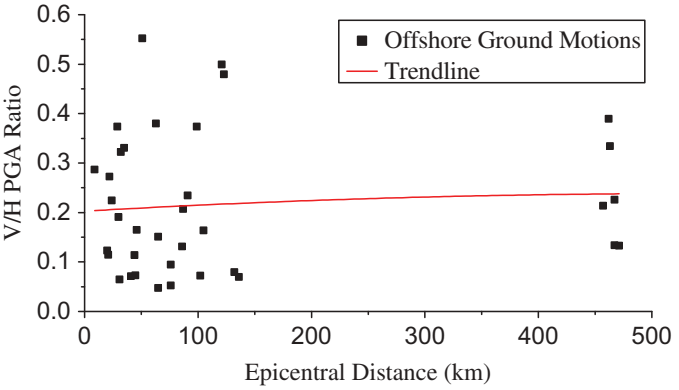

FIGURE 21 Relationship between the epicentral distance and the V/H PGA ratio for offshore ground motions in the K-net.

ratio increases slightly with increasing epicentral distance, but the change is not obvious and the ratio ranges between 0.2 and 0.25.

The relationships between the earthquake magnitude and the average V/H PGA ratio for each earthquake are shown in Fig. 22. Furthermore, the data were classified according to whether the hypocenter was located on the seafloor or on land. It could be found that there was no obvious regularity between the V/H PGA ratio and the earthquake magnitude; perhaps this is because of the lack of enough earthquake events selected for this study. However, the V/H PGA ratio for offshore ground motions from earthquakes occurring on the seafloor was higher than that occurring on land. The V/H PGA ratio for offshore ground motions from earthquakes occurring on the seafloor was between 0.2 and 0.28; while the ratio for ground motions from earthquakes occurring on land ranged between 0.15 and 0.2.

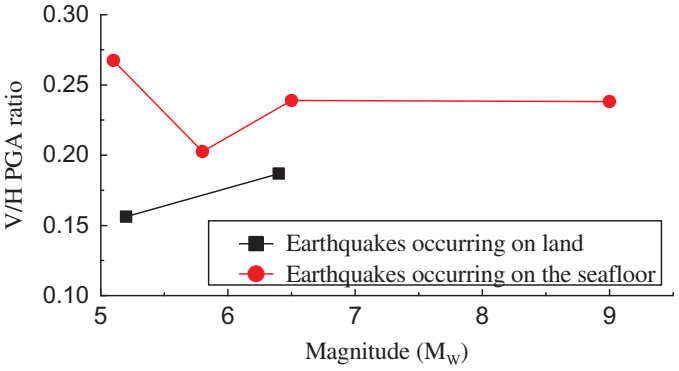

FIGURE 22 Relationship between the earthquake magnitude and the V/H PGA ratio for offshore ground motions in the K-net.

4.2. Vertical-to-Horizontal Response Spectral Ratio

By calculating the vertical and horizontal acceleration response spectra respectively, the vertical-to-horizontal response spectral ratio (V/H RS ratio) can be obtained by taking the vertical response spectral values divided by horizontal response spectral values. Further, the V/H RS ratio is plotted as a curve to represent the relationship between the response spectral ratio and the period. The V/H RS ratios for onshore and offshore ground motions during six earthquakes and the corresponding coefficient of variation are shown in Figs. 23–28. It illustrates that the V/H RS ratios for ground motions were found to be similar in different earthquake events. The differences in the V/H RS ratios between onshore and offshore ground motions are summarized as follows. For periods less than 1 s, the V/H RS ratio for offshore ground motions was lower than that of onshore ground motions. Especially for short periods less than 0.5 s, the V/H RS ratio for offshore ground motions was between 0.2 and 0.4; this is about 30% to 50% of the V/H RS ratio for onshore ground motions. For periods between 0.5 and 1.5 s, the V/H RS ratio for offshore ground motions

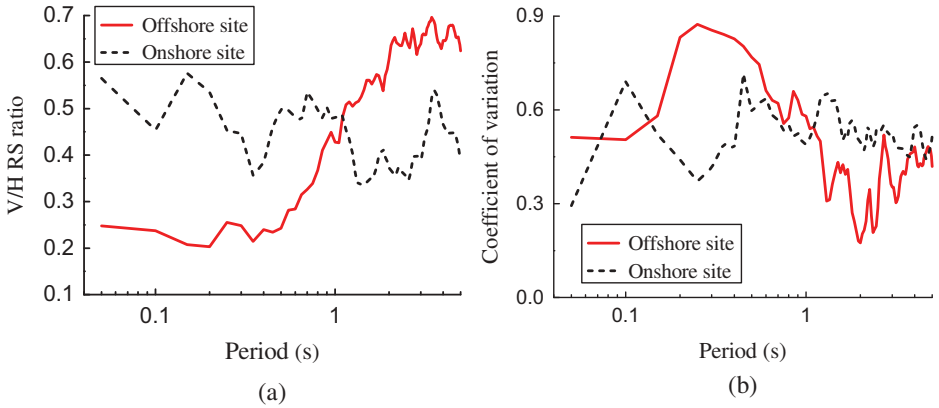

FIGURE 23 Vertical-to-horizontal response spectral ratios for onshore and offshore ground motions from the K-net in the earthquake on April 21, 2006 and corresponding coefficient of variation.

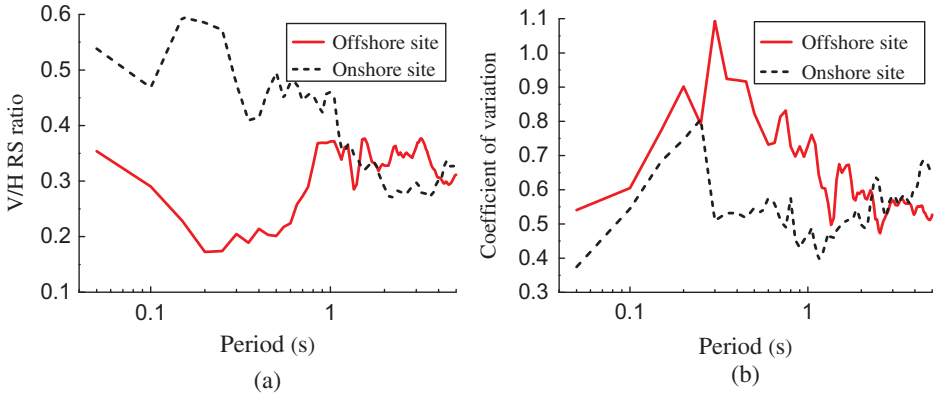

FIGURE 24 Vertical-to-horizontal response spectral ratios for onshore and offshore ground motions from the K-net in the earthquake on May 2, 2006 and corresponding coefficient of variation.

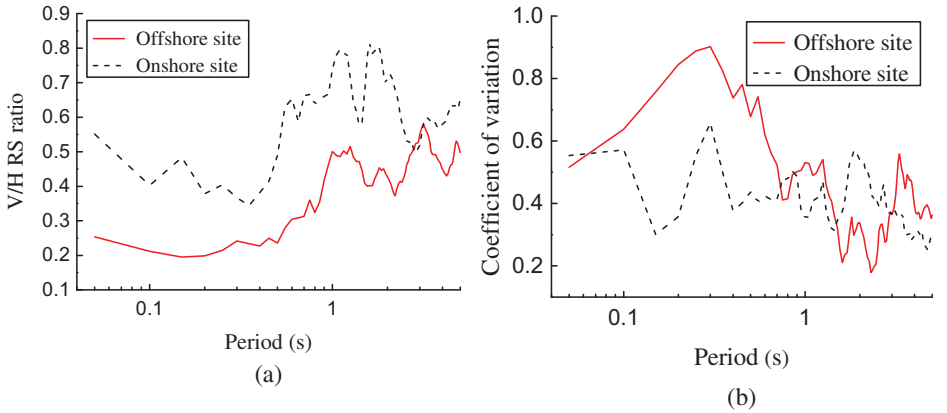

FIGURE 25 Vertical-to-horizontal response spectral ratios for onshore and offshore ground motions from the K-net in the earthquake on August 11, 2009 and corresponding coefficient of variation.

increased rapidly. For periods longer than 1.5 s, the V/H RS ratio for offshore ground motions was close to or exceeded the V/H RS ratio for onshore ground motions.

With regard to a low V/H RS ratio for offshore ground motion for periods less than 1 s, a water layer may play an important role. Several theoretical analyses for the effect of sea water on vertical ground motions at offshore sites have been provided.

Crouse and Quilter [1991] built a simple model of a water layer overlying an elastic half space, subjected to a vertical incident plane P-wave. This study presented that the largest effect of a water layer on the vertical ground motion should be at frequencies corresponding to P-wave resonance in the water layer.

Using the similar model of Crouse and Quilter, the effect of seawater on inclined incident plane P and SV waves are discussed by Diao *et al.* [2014]. They found that a water layer can reduce the vertical motion at P-wave resonance frequencies in the water, and the effect of water layer on vertical motion is dependent on the impedance ratio between the seawater and the underlying medium.

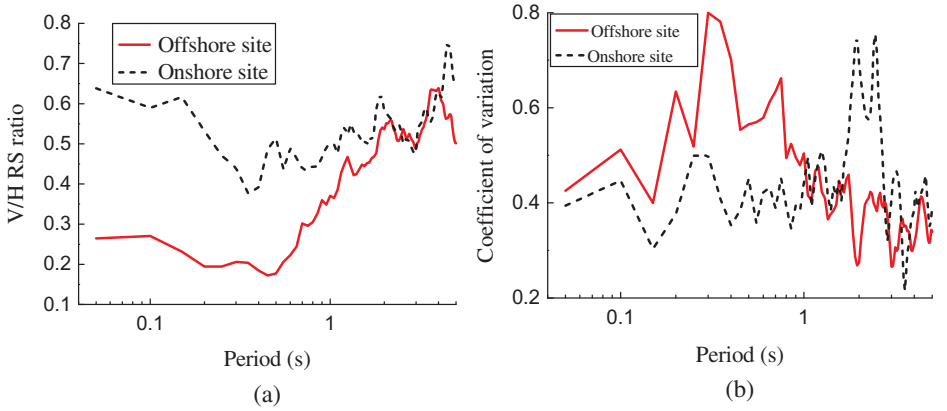

FIGURE 26 Vertical-to-horizontal response spectral ratios for onshore and offshore ground motions from the K-net in the earthquake on March 11, 2011 and corresponding coefficient of variation.

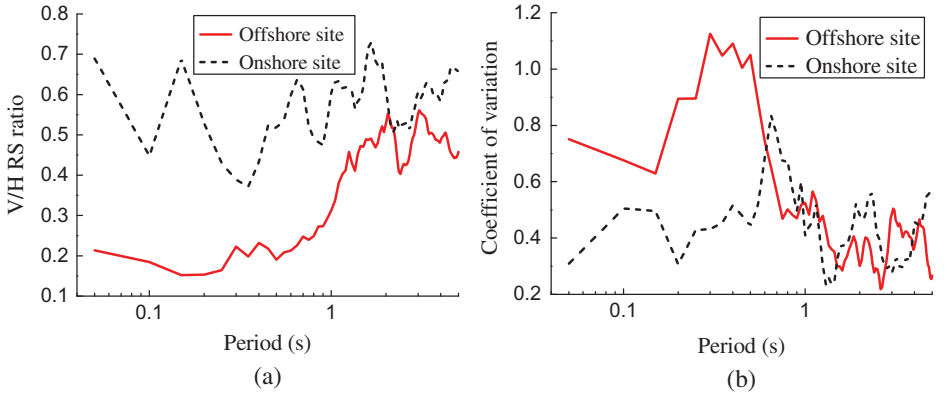

FIGURE 27 Vertical-to-horizontal response spectral ratios for onshore and offshore ground motions from the K-net in the earthquake on March 15, 2011 and corresponding coefficient of variation.

Based on the offshore ground motion records from the SEMS, Boore and Smith [1999] found that the V/H ratios of the Fourier amplitude spectra (or PSV response spectra) for offshore ground motions were much smaller than those of onshore ground motions at relatively high frequencies (above about 3 Hz). A numerical model was built to explain the particular observed ratios and it was concluded that the water can reduce vertical ground motions at resonant frequencies of vertically propagating P-waves in the water layer [see Figs.18 and 19 in Boore and Smith, 1999].

The average V/H RS ratio of all the ground motions from the K-net and SEMS are compared in Fig. 29a. It is found that the V/H RS ratio for offshore ground motions from the SEMS was similar to that of the K-net, illustrating that the water layer can reduce the V/H RS ratios for offshore ground motions in both the K-net and SEMS. Because the water depths above the K-net sites are much greater than the SEMS, the water depth seems to have little influence on the V/H RS ratio for offshore ground motions.

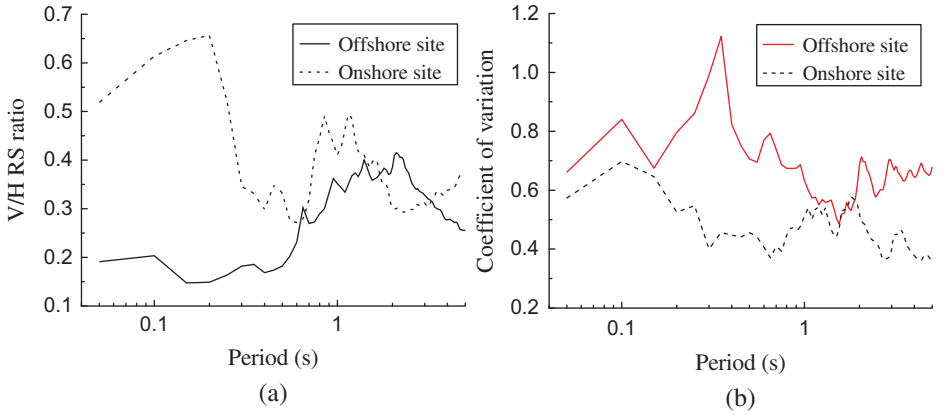

FIGURE 28 Vertical-to-horizontal response spectral ratios for onshore and offshore ground motions from the K-net in the earthquake on July 3, 2012 and corresponding coefficient of variation.

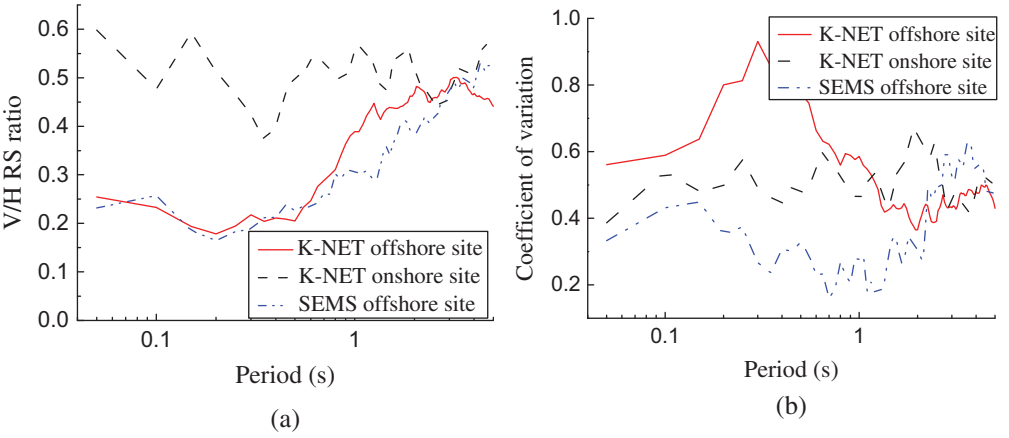

FIGURE 29 average vertical-to-horizontal response spectral ratios for onshore and offshore ground motions from the K-net and SEMS and corresponding coefficient of variation.

Things are not as simple as that; for example, the V/H RS ratios for offshore ground motions at KNG202, KNG203, and KNG205 sites in the K-net and the average V/H RS ratio in SEMS are compared with each other in Fig. 30. The water depths of the KNG202, KNG203, and KNG205 stations are 2339, 902, and 1486 m, respectively. Figure 30 shows that the V/H RS ratios at KNG202 site were greater than those at KNG203 and KNG205 sites for periods less than about 0.8 s. Ratios at KNG203 and KNG205 sites were almost similar to those in the SEMS for periods less than about 0.8 s in spite of their different water depths.

Through observing the V/H RS ratios at the same offshore site in the K-net, it is found that the regularity of the V/H RS ratios at the same offshore site for different earthquakes was similar. Due to the ratio of vertical-to-horizontal response spectra (V/H RS ratio) should remove all influencing factors (earthquake magnitude, type of faulting, and

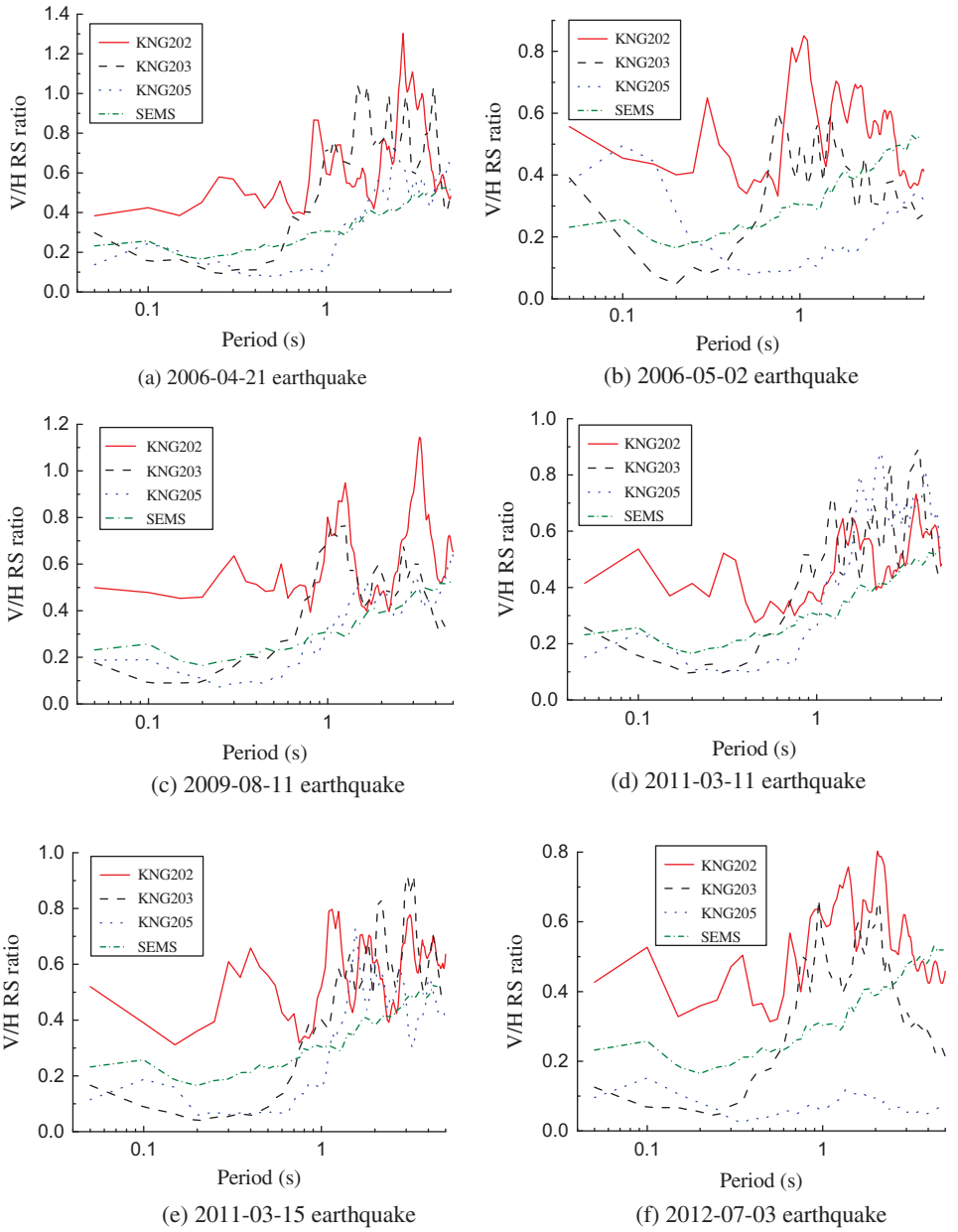

FIGURE 30 Vertical-to-horizontal response spectral ratios for offshore ground motions at KNG202, KNG203, and KNG205 stations and the V/H RS ratio for offshore ground motions in the SEMS.

propagation path etc.) but the effect of local geology [Atakan and Havskov, 1996], it indicates that the local site condition at the offshore sites could influence the V/H RS ratio for offshore ground motions. Therefore more discussions should be made.

More specifically, it was mentioned previously that the largest effect of the water layer on the vertical ground motion should be at the resonance frequencies of the water layer. The resonance frequencies are given as follows:

$$f_n = \frac{C}{4H}n, \tag{4}$$

where C is the P-wave velocity in water (about 1500 m/s), H is the water depth, and n is an odd number (1, 3, 5, and 7 . . .) [Crouse and Quilter, 1991]. For example, the water depth of one offshore sites is about 60 m in the SEMS, this gives f1 = 6.25 Hz (at short period 0.16 s), where the resonance frequency is at high frequency zones.

The water depth at offshore sites in the K-net is between 900 and 2300 m. When water depth is H = 1486 m (KNG205), it gives the resonance frequencies f1 = 0.25 Hz (T = 4.0 s), f3 = 0.76 Hz (T = 1.31 s), f5 = 1.26 Hz (T = 0.79 s), f7 = 1.77 Hz (T = 0.56 s), and f9 = 2.27 Hz (T = 0.44 s). The above theory calculation indicates that the deep water layer above the offshore sites in the K-net should reduce the vertical ground motion not only at high frequencies (short periods), but also at lower frequencies (long periods). As shown in Figs. 23–29, the V/H RS ratios for offshore ground motions are much lower than those of onshore ground motions at short periods (high frequencies). But comparing to onshore ground motions, the V/H RS ratios for offshore ground motions have not been reduced obviously at long periods (low frequencies). The reasons may be caused by that the vertical ground motion usually has more high frequency contents; as such the effect of the water layer can only work at high order resonant frequencies. Furthermore, the water depths of the offshore sites are different with each other; this may cause that the resonant frequencies for the offshore ground motions at different sites are not the same. Therefore, the effects of a water layer on statistical average V/H RS ratios may be weaken.

To summarize, the V/H RS ratio for offshore ground motions should be reduced by water layer. Furthermore, the local site condition and the water depth may also affect the V/H RS ratio for offshore ground motions.

Boore and Smith [1999] also pointed out that the characteristics of the offshore ground motions at lower frequencies (longer periods) are due to the site condition (low shear wave velocity) beneath the seafloor, rather than the effect of a water layer.

The statistical coefficients of variation of the normalized response spectra for onshore and offshore ground motions were almost smaller than 1.0 in Figs. 23b–29b. The coefficient of variation of the onshore data was smaller.

4.3. Influence of the Epicentral Distance

The V/H RS ratios for onshore and offshore ground motions in MSR, MMR, and GFR the groups are shown in Figs 31a–33a. The V/H RS ratio for offshore ground motions in 3 groups from the K-net and 1 group from the SEMS are compared with each other in Fig. 34a. The curves of the V/H RS ratio with different epicentral distances were found to be similar in a moderate earthquake (MSR, MMR, and SEMS group), which indicates that the epicentral distance has little influence on the V/H RS ratio for offshore ground motion in a moderate earthquake. The V/H RS ratio for offshore ground motions in the GFR group was larger for periods longer than 1 s.

The statistical coefficients of variation of the normalized response spectra for onshore and offshore ground motions are smaller than 1.0 in Figs. 31b–34b. The coefficient of variation for the SEMS data is smaller than 0.6 in Fig. 34b.

5. Conclusions

Some onshore and offshore ground motions were recorded simultaneously in the K-net network. Using these records and the offshore ground motion records in the SEMS,

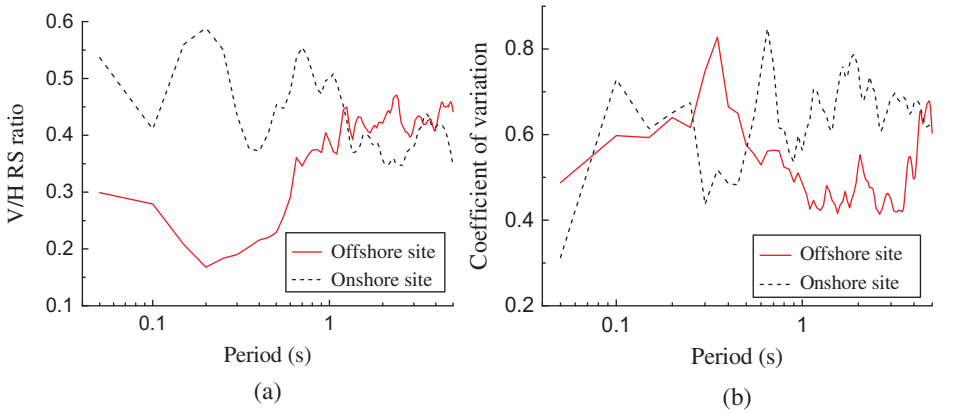

FIGURE 31 Vertical-to-horizontal response spectral ratios for onshore and offshore ground motions in MSR group and corresponding coefficient of variation.

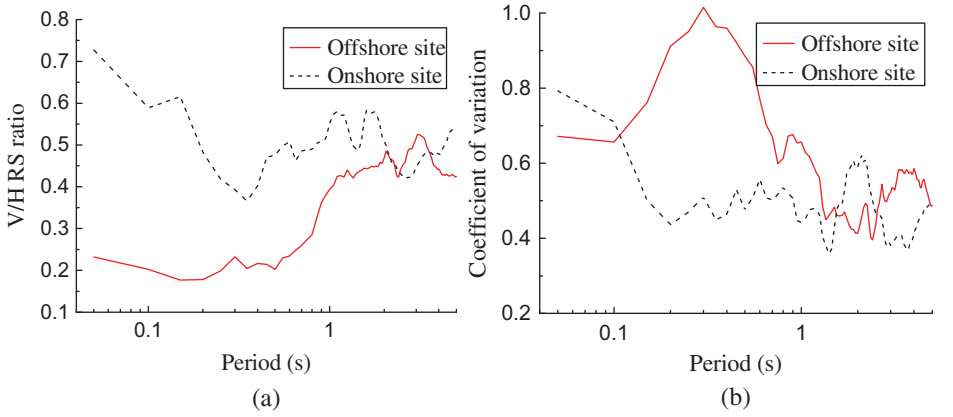

FIGURE 32 Vertical-to-horizontal response spectral ratios for onshore and offshore ground motions in MMR group and corresponding coefficient of variation.

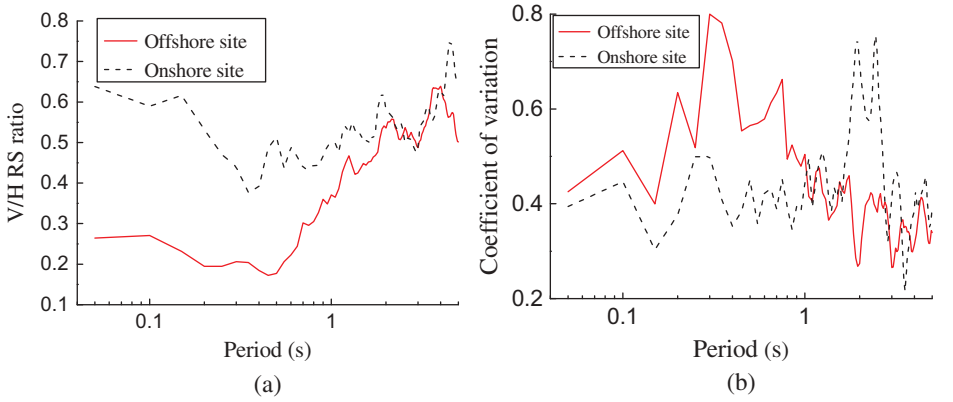

FIGURE 33 Vertical-to-horizontal response spectral ratios for onshore and offshore ground motions in GFR group and corresponding coefficient of variation.

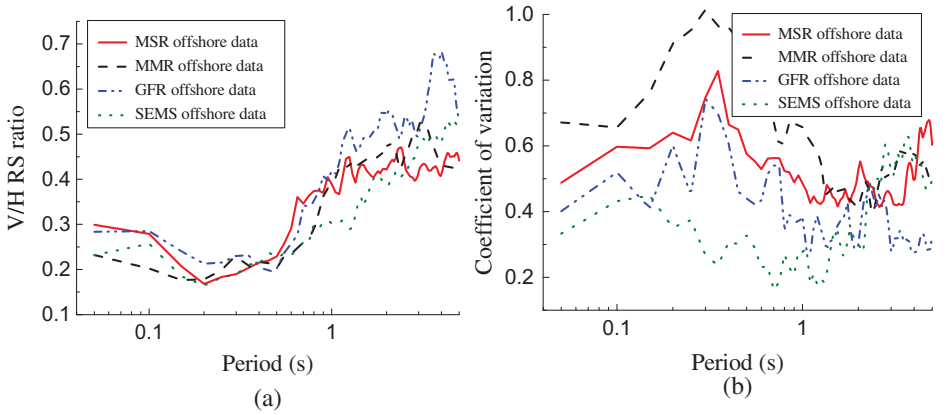

FIGURE 34 Vertical-to-horizontal response spectral ratios for offshore ground motions with different epicentral distances from the K-net and SEMS and corresponding coefficient of variation.

a comparison of the characteristics between onshore and offshore ground motion is summarized.

In general, the horizontal normalized response spectra for offshore ground motions had a wider peak platform than that of onshore ground motions. The characteristic period of the former (0.5–0.6 s) was larger than the latter (0.2–0.3 s). For periods between 0.2 and 1 s, the spectral values for offshore ground motions were larger than those of onshore ground motions. A deep deposition layer is commonly covered on the seafloor and may be the reason for the differences in the horizontal response spectra.

The epicentral distances had a significant influence on the horizontal response spectra for offshore ground motions in a moderate earthquake; namely, the larger the epicentral distance, the larger the characteristic period. The spectral values for offshore ground motion in a great earthquake with far epicentral distance will be larger at long periods.

The horizontal normalized response spectra for offshore ground motions from the SEMS were consistent with that of the K-net. Further, the depth of the offshore stations under the water layer in the K-net is significantly larger than that of the SEMS, indicating that the influence of the water depth on the horizontal response spectra of offshore ground motions is little.

The vertical PGA at the offshore sites was significantly lower than that at onshore sites. The epicentral distance and the earthquake magnitude had little influence on the V/H PGA ratio, but the V/H PGA ratio may be influenced by an earthquake occurring on the seafloor or on land.

The V/H RS ratio for offshore ground motion was much lower than that of onshore ground motion, especially for short periods lower than 1 s. The reason for this may be that the vertical ground motion can be reduced by the water layer at the frequencies corresponding to P-wave resonant in the water layer. Furthermore, the local site condition under seafloor may also influence the V/H RS ratio for the offshore ground motion. The influence of the epicentral distance on the V/H RS ratio is not obvious in a moderate earthquake. Moreover, the effect of the water depth on vertical ground motion should be further investigated.

Acknowledgments

We thank the K-net strong-motion seismograph network for sharing their data. We thank the anonymous referees for their detailed comments that helped to improve this article substantially.

Funding

This research was supported by the National Basic Research Development Program of China (973 Program) (No. 2011CB013605), National Natural Science Foundation of China under Grant (Nos. NNSFC51178071 and NNSFC51008041), and Program for New Century Excellent Talents in University of Ministry of Education of China under Grant (No.CET-12-0751).

References

Ambraseys, N. N. and Douglas, J. [2003] "Near-field horizontal and vertical earthquake ground motions," *Soil Dynamics and Earthquake Engineering* **23**(1), 1–18.

Atakan, K. and Havskov, L. [1996] "Local site effects in the northern North Sea based on single-station spectral ratios of OBS recordings," *Terra Nova* **8**(1), 22–33.

Aoi, S., Kunugi, T., and Fujiwara, H. [2004] "Strong-motion seismograph network operated by NIED: K-net and Kik-net," *Journal of Japan Association for Earthquake Engineering* **4**(3), 65–74.

Bindi, D., Luzi, L., Massa, M., and Pacor, F. [2010] "Horizontal and vertical ground motion prediction equations derived from the Italian Accelerometric Archive (ITACA)," *Bulletin of Earthquake Engineering* **8**(5), 1209–1230.

Boore, D. M. and Bommer, J. J. [2005] "Processing of strong-motion accelerograms: Needs, options and consequences," *Soil Dynamics and Earthquake Engineering* **25**, 93–115.

Boore, D. M. and Smith, C. E. [1999] "Analysis of earthquake recordings obtained from the Seafloor Earthquake Measurement System (SEMS) instruments deployed off the coast of southern California," *Bulletin of the Seismological Society of America* **89**(1), 260–274.

Bozorgnia, Y., Campbell, K. W., and Niazi, M. [2000] "Observed spectral characteristics of vertical ground motion recorded during worldwide earthquakes from 1957 to 1995," *Proc. of the 12th World Conference on Earthquake Engineering* **2671**(4), New Zealand: [sn].

Chopra, A. K. [2007] "Elastic response spectrum: A historical note," *Earthquake Engineering and Structure Dynamics* **36**(1), 3–12.

Crawford, W. C., Webb, S. C. and Hildebrand, J. A. [1991] "Seafloor compliance observed by long-period pressure and displacement measurements," *Journal of Geophysical Research: Solid Earth (1978–2012)* **96**(B10), 16151–16160.

Crouse, C. B. and Quilter, J. [1991] "Seismic hazard analysis and development of design spectra for Maul A platform," *Proc. Pacific Conference on Earthquake Engineering*, **III**, New Zealand, pp. 137–148.

Diao, H., Hu, J., and Xie, L. [2014] "Effect of seawater on incident plane P and SV waves at ocean bottom and engineering characteristics of offshore ground motion records off the coast of southern California, USA," *Earthquake Engineering and Engineering Vibration* **13**(2), 181–194.

Dimitriu, P., Kalogeras, I., and Theodulidis, N. [1999] "Evidence of nonlinear site response in horizontal-to-vertical spectral ratio from near-field earthquakes," *Soil Dynamics and Earthquake Engineering* **18**(6), 423–435.

Elgamal, A. and He, L. [2004] "Vertical earthquake ground motion records: an overview," *Journal of Earthquake Engineering* **8**(5), 663–697.

Fujiwara, H., Aoi, S., Kunugi, T., and Adachi, S. [2004] "Strong-motion Observation Networks of NIED: K-NET and KiK-net," *Processing of the COSMOS Workshop on Strong-Motion Record, Cosmos publication no CP-2004/02*.

Hashimoto, K. and Chouw, N. [2003] "Investigation of the effect of Kobe earthquake on a three-dimensional soil–structure system," *JSCE Journal of Earthquake Engineering* **27**, 1–8.

Kim, S. J., Holub, C. J., and Elnashai, A. S. [2010] "Analytical assessment of the effect of vertical earthquake motion on RC bridge piers," *Journal of Structural Engineering* **137**(2), 252–260.

KomakPanah, A. and Bagheri, M. [2013] "Evaluation of Aa And Av coefficients in Iran for limited displacement design method of retaining walls," *Journal of Seismology and Earthquake Engineering* **14**(3), 207–217.

Lussou, P., Bard, P. Y., Cotton, F., and Fukushima, Y. [2001] "Seismic design regulation codes: contribution of K-net data to site effect evaluation," *Journal of Earthquake Engineering* **5**(1), 13–33.

Mendes, N. and Lourenço, P. B. [2009] "Seismic assessment of masonry "Gaioleiro" buildings in Lisbon, Portugal," *Journal of Earthquake Engineering* **14**(1), 80–101.

Nakamura, Y. [1989] "A method for dynamic characteristics estimation of subsurface using microtremor on the ground surface," *Quarterly Reports*, Railway Technical Research Institute, **30**(1).

Nolen-Hoeksema, S. and Morrow, J. [1991] "A prospective study of depression and posttraumatic stress symptoms after a natural disaster: the 1989 Loma Prieta Earthquake," *Journal of Personality and Social Psychology* **61**(1), 115–121.

Okada, Y., Kasahara, K., Hori, S., Obara, K., Sekiguchi, S., Fujiwara, H., and Yamamoto, A. [2004] "Recent progress of seismic observation networks in Japan—Hi-net, F-net, K-NET and KiK-net," *Earth Planets Space* **56**(8), xv–xxviii.

Otsuka, K. [1985] "Processes and faces of active trough filling up sediments-geology of upper quaternary sediments in the northernmost areas of the Sagami and Suruga Troughs," *Geosciences Reports*, Shizuoka University, pp. 57–117. (In Japanese)

Pousse, G., Berge-Thierry, C., Bonilla, L. F., and Bard, P. Y. [2005] "Eurocode 8 design response spectra evaluation using the K-net Japanese database," *Journal of Earthquake Engineering* **9**(04), 547–574.

Smith, C. E. [1994] "Dynamic response of offshore steel-jacket platforms subject to measured seafloor seismic ground motions," Ph.D. thesis, George Washington University, Washington.

Takao, E., Yukio F., Eisuke, F., Sin-Iti, I., Isao, W., and Hiroyuki, F. [1998] "A real-time observation network of ocean-bottom-seismometers deployed at the Sagami trough subduction zone, central Japan," *Marine Geophysical Researches* **20**, 73–94.

Tanaka, Y. [2000] "The 1995 great Hanshin earthquake and liquefaction damages at reclaimed lands in Kobe Port," *International Journal of Offshore and Polar Engineering* **10**(1), 15–25.

Tsai, N. C. [1970] "A note on the steady-state response of an elastic half-space," *Bulletin of the Seismological Society of America* **60**(3), 795–808.

Yanf, J. and Lee, C. M. [2007] "Characteristics of vertical and horizontal ground motions recorded during the Niigataken Chuetsu Japan Earthquake of 23 October 2004," *Engineering Geology* **94**(1/2), 50–64.

APPENDIX: Data of Ground Motions

APPENDIX A1 Data of ground motions for the earthquake on April 21, 2006 (A group: offshore stations; B group: onshore stations)

Code	Station name	PGA (gal)			Epicentral distance (km)	$\bar{V}_s$ (m/s) and Depth (m)
		EW horizontal	NS horizontal	Vertical		
A1	KNG201	123.268	65.005	4.940	76	No data
A2	KNG202	37.017	22.455	11.296	63	No data
A3	KNG203	84.955	38.873	7.051	44	No data
A4	KNG204	52.418	39.795	15.227	35	No data
A5	KNG205	251.703	145.940	22.788	21	No data
A6	KNG206	119.569	81.320	22.542	24	No data
B1	SZO001	209.613	99.552	37.941	25	292/10
B2	SZO002	311.747	127.688	101.815	8.8	243/12
B3	SZO007	130.721	144.957	37.854	23	343/10
B4	TKY008	80.523	92.359	35.427	25	377/20
B5	TKY010	44.237	21.609	14.268	63	258/20

*Data in Appendix A can be found on the website: http://www.kyoshin.bosai.go.jp/

APPENDIX A2 Data of ground motions for the earthquake on May 2, 2006 (A group: offshore stations; B group: onshore stations)

Code	Station name	PGA (gal)			Epicentral distance (km)	$\bar{V}_s$ (m/s) and Depth (m)
		EW horizontal	NS horizontal	Vertical		
A1	KNG201	36.367	34.106	1.659	65	No data
A2	KNG202	24.845	22.287	13.008	51	No data
A3	KNG203	175.713	98.423	44.210	32	No data
A4	KNG204	101.279	104.738	28.061	22	No data
A5	KNG205	418.672	252.064	96.225	8.8	No data
A6	KNG206	233.129	77.748	19.095	20	No data
B1	KNG008	22.613	11.104	4.386	73	275/20
B2	SZO001	126.390	66.322	15.975	34	292/10
B3	SZO002	222.863	77.238	51.065	21	243/12
B4	TKY008	59.621	104.257	55.788	16	377/20
B5	TKY010	13.947	12.933	8.118	60	258/20

APPENDIX A3 Data of ground motions for the earthquake on August 11, 2009 (A group: offshore stations; B group: onshore stations)

Code	Station name	PGA (gal)			Epicentral distance (km)	$\bar{V}_s$ (m/s) and Depth (m)
		EW horizontal	NS horizontal	Vertical		
A1	KNG201	27.571	34.850	2.469	132	No data
A2	KNG202	17.477	15.402	7.881	123	No data
A3	KNG203	34.050	35.467	5.688	105	No data
A4	KNG204	20.806	25.566	8.662	99	No data
A5	KNG205	56.366	47.886	6.839	86	No data
A6	KNG206	89.002	94.936	19.046	87	No data
B1	KNG008	36.134	26.921	16.656	116	275/20
B2	SZO001	135.626	129.990	30.631	66	292/10
B3	SZO002	131.382	175.297	46.395	59	243/12
B4	TKY009	66.717	57.996	21.930	87	283/20
B5	TKY010	51.187	73.723	38.325	83	258/20

APPENDIX A4 Data of ground motions for the earthquake on March 11, 2011 (A group: offshore stations; B group: onshore stations)

Code	Station name	PGA (gal)			Epicentral distance (km)	$\bar{V}_s$ (m/s) and Depth (m)
		EW horizontal	NS horizontal	Vertical		
A1	KNG201	123.835	107.079	15.315	471	No data
A2	KNG202	149.993	94.919	47.687	462	No data
A3	KNG203	90.94	69.20	18.095	467	No data
A4	KNG204	65.196	59.817	20.874	463	No data
A5	KNG205	150.154	157.687	20.597	467	No data
A6	KNG206	367.516	208.749	61.542	457	No data
B1	CHB017	90.356	108.531	38.945	399	218/20
B2	KNG008	115.522	95.731	48.525	422	275/20
B3	SZO001	49.694	28.325	11.870	472	292/10
B4	SZO002	74.741	43.712	17.767	485	243/12
B5	TKY009	23.855	23.885	13.516	488	283/20
B6	TKY010	213.399	235.792	134.635	526	258/20

APPENDIX A5 Data of ground motions for the earthquake on March 15, 2011 (A group: offshore stations; B group: onshore stations)

Code	Station name	PGA (gal) EW horizontal	PGA (gal) NS horizontal	PGA (gal) Vertical	Epicentral distance (km)	$\bar{V}_s$ (m/s) and Depth (m)
A1	KNG201	46.500	33.376	2.791	136	No data
A2	KNG202	24.063	14.840	9.716	121	No data
A3	KNG203	84.538	76.398	5.815	102	No data
A4	KNG204	40.794	22.652	7.429	91	No data
A5	KNG205	105.443	101.926	9.780	76	No data
A6	KNG206	103.410	70.254	13.106	65	No data
B1	CHB017	12.639	13.655	7.344	124	218/20
B2	KNG008	37.373	51.832	29.215	63	275/20
B3	SZO001	194.106	68.706	29.868	38	292/10
B4	SZO002	36.836	46.340	20.850	52	243/12
B5	TKY008	29.184	29.180	11.715	85	377/20

APPENDIX A6 Data of ground motions for the earthquake on July 3, 2012 (A group: offshore stations; B group: onshore stations)

Code	Station name	PGA (gal) EW horizontal	PGA (gal) NS horizontal	PGA (gal) Vertical	Epicentral distance (km)	$\bar{V}_s$ (m/s) and Depth (m)
A1	KNG201	83.132	91.948	6.360	45	No data
A2	KNG202	135.746	106.527	45.247	29	No data
A3	KNG203	70.773	86.059	5.082	31	No data
A4	KNG204	56.191	54.516	10.545	30	No data
A5	KNG205	155.703	170.789	11.606	41	No data
A6	KNG206	118.567	74.272	15.893	46	No data
B1	CHB017	44.213	25.101	16.007	38	218/20
B2	KNG008	12.006	14.327	16.318	81	275/20
B3	SZO001	38.964	22.274	5.662	74	292/10
B4	SZO002	52.635	22.212	26.809	70	243/12
B5	TKY009	36.363	34.030	14.856	52	283/20

APPENDIX B Data of offshore ground motions in the SEMS

Earthquake ID	Station name	PGA (gal)			Epicentral distance (km)
		Horizontal-x	Horizontal-y	Vertical	
SB81	S1HN	15.873	21.379	3.813	86.0
NP86	S2EE	30.135	17.89	3.109	147.5
OS86	S2EE	18.500	28.175	3.679	72.5
UP90	S3EE	14.902	27.683	3.636	74.4
RC95	S4IR	0.455	0.368	0.121	309.1
CL97	S4GR	0.436	0.379	0.128	258.1
S97A	S4GR	1.814	2.145	0.384	76.7
S97A	S4IR	0.358	0.335	0.075	191.2
S97B	S4GR	0.554	0.770	0.136	79.3

*The shear-wave velocities beneath the SEMS offshore sites are about 220 m/s [Boore and Smith, 1999]